Original Paper

A deep-learning-based prediction method of the estimated ultimate recovery (EUR) of shale gas wells

Yu-Yang Liu [a, b, *], Xin-Hua Ma [a, b, **], Xiao-Wei Zhang [a, b], Wei Guo [a, b], Li-Xia Kang [a, b], Rong-Ze Yu [a, b], Yu-Ping Sun [a, b]

[a] PetroChina Research Institute of Petroleum Exploration and Development (RIPED), Beijing, 100083, China
[b] China National Shale Gas Research & Development (Experiment) Center, Langfang, 065007, Hebei, China

ARTICLE INFO

ABSTRACT

The estimated ultimate recovery (EUR) of shale gas wells is influenced by many factors, and the accurate prediction still faces certain challenges. As an artificial intelligence algorithm, deep learning yields notable advantages in nonlinear regression. Therefore, it is feasible to predict the EUR of shale gas wells based on a deep-learning algorithm. In this paper, according to geological evaluation data, hydraulic fracturing data, production data and EUR evaluation results of 282 wells in the WY shale gas field, a deep-learning-based algorithm for EUR evaluation of shale gas wells was designed and realized. First, the existing EUR evaluation methods of shale gas wells and the deep feedforward neural network algorithm was systematically analyzed. Second, the technical process of a deep-learning-based algorithm for EUR prediction of shale gas wells was designed. Finally, by means of real data obtained from the WY shale gas field, several different cases were applied to testify the validity and accuracy of the proposed approach. The results show that the EUR prediction with high accuracy. In addition, the results are affected by the variety and number of input parameters, the network structure and hyperparameters. The proposed approach can be extended to other shale fields using the similar technic process.

1. Introduction

As exploration and development processes continuously advance, the contradiction between oil and gas resources has become increasingly notable. Meanwhile, the development prospects of unconventional oil and gas resources are progressively highlighted (Dong et al., 2016; Liu et al. 2019a, 2019b, 2020; Zou et al. 2015, 2016, 2019, 2019). With the shale gas revolution in North America and the continuous optimization of the energy structure, shale gas, as an unconventional oil and gas resource, has become one of the important pillars of the increase in reserves and enhancement of the production of oil and gas resources in China and even worldwide in the future (Dong et al., 2012; Ma, 2017a, 2017b; Ma and Xie, 2018). Large-scale horizontal well and multistage hydraulic fracturing have been usually adopted in shale gas wells to obtain the maximum economic benefits (Ma, 2018; Zhao et al., 2020).

The estimated ultimate recovery (EUR) of shale gas wells determines the life cycle of their development, and it is also one of the most important parameters of shale gas wells establishing their economic benefits. Due to varying geological conditions, construction conditions, production systems, etc., the EUR of many different shale gas wells in similar areas or the same area largely differs, and even the EUR of many horizontal shale gas wells completed on the same drilling platform is also quite different. Therefore, the rapid, effective, reasonable and accurate EUR prediction of shale gas wells is facing great challenges by the control of a series of factors.

EUR evaluation methods of shale gas wells mainly include the empirical production decline method, modern production decline method (including the flow material balance method), simulation prediction method (analytical model method and numerical simulation method) and probability method (Bi et al., 2020; Zhao et al., 2019; Zhang et al. 2018, 2020). The deep learning algorithm has been adopted in EUR prediction of natural gas wells, but for

shale gas wells, the current research is limited, and most studies still mainly apply conventional methods such as empirical production decline curves to perform EUR prediction.

Researchers have also achieved a series of improvements in the EUR prediction for shale gas wells. Knowledge-driven approaches are the main EUR prediction in shale gas development practice. Coupled parameters such as normalized production and pressure data are applied to predict the EUR of shale gas wells and successfully applied this approach in the Zhaotong and Changning-Weiyuan shale gas demonstration zone in China (Zhang et al. 2018, 2020). A quick EUR evaluation method for shale gas wells under variable production rates based on data noise reduction is developed to improve the EUR prediction accuracy (Zhao et al., 2019). In the above attempts, analysis and optimization are conducted based on the conventional production law of shale gas wells, and most of these methods are knowledge-driven EUR evaluation methods of shale gas wells (Zhang et al. 2018, 2020; Zhao et al., 2019). There are only a few attempts at deep learning-based or data-driven EUR evaluation methods. Bi et al. selected the Changning shale gas demonstration zone in China as an example and implemented the probability method to estimate the EUR value of undeveloped areas based on the EUR value of developed areas with similar geological and engineering conditions, thereby revealing that under similar geological and engineering conditions, in the absence of interaction among wells, the production laws in developed and undeveloped areas are similar, and the EUR of shale gas wells in undeveloped areas could be calculated by means of certain relevant parameters of developed areas (Bi et al., 2020). By means of a data-driven method, Hector and Horacio adopted a deep convolutional neural network to predict unconventional shale reservoir behavior, and the matching degree between their prediction and actual results was relatively high (Hector and Horacio, 2020). It shows the potentials of deep-learning in shale gas EUR prediction.

The above studies also indicate that a certain theoretical basis and application foundation are generated by evaluating the EUR of undeveloped areas by means of the integration of geological factors, engineering factors, production factors and other constraints and the deep learning algorithm to establish the EUR evaluation model of developed areas.

A deep learning algorithm is an algorithm that learns from data, and it extracts corresponding patterns from a variety of complex raw data. With the continuous improvement in computing power, researchers have applied deep learning algorithms in various fields such as rock type division (Arns et al., 2001; Ismail et al., 2013; Ismail, 2014; Yang et al., 2017), prediction of rock reservoir parameters (Iturrar and Parra, 2014; Zerrouki et al., 2014), determination of the boundaries of sedimentary facies and lithofacies (Liu et al., 2017b; Singh, 2011; Silversides et al., 2015), restoration and reconstruction of logging curves (Alizadeh et al., 2012; Rolon et al., 2009; Salehi et al., 2016), establishment and simulation of digital cores (Liu and Pan, 2017; Liu et al., 2017a; Wang et al., 2019c), production history matching of oil and gas wells (Zhou, 2017; Xu, 2018; Liu et al., 2021) and calculation of shale gas reservoir's characteristics like TOC and gas content (Wang et al., 2019a; Zhu et al. 2019, 2020a, 2020b), which has resolved the problems of related scientific research and engineering practices in the process of oil and gas production, thereby demonstrating the great potential of deep learning algorithms in the oil and gas field.

The geological factor of shale gas reservoirs is one of the key factors controlling the EUR of shale gas wells. The effective thickness, organic matter maturity and matrix porosity of shale reservoirs directly affect the corresponding shale gas reserves. The engineering factor of shale gas wells is another main factor controlling the EUR of shale gas wells. The horizontal section length,

drill-in rate of high-quality reservoirs, number and length of fracturing sections and hydraulic fracture length of shale gas wells control the output of shale gas. The production factor of shale gas wells is the final main factor influencing the EUR of shale gas. Parameters such as the test output and average daily output in the first year are also related to the EUR of shale gas wells. Joint control of the above factors determines the EUR of shale gas wells.

Based on the existing attempts of researchers, this paper predicts the EUR of shale gas wells by means of a deep learning algorithm, the deep feedforward neural network in detail, and integration of geological factors, engineering factors, production factors and other constraints. The structure of the paper is as follows: first, the basic mathematical background of gas well EUR evaluation and the deep feedforward neural network is introduced; second, the EUR evaluation method of shale gas wells with the deep feedforward neural network is designed and realized; then, the feasibility and accuracy of the method are systematically analyzed through real data of marine shale gas wells in the WY shale gas field of the Sichuan Basin, China; and finally, based on the above results, conclusions are obtained.

2. Basic mathematical background

2.1. Conventional EUR evaluation method of shale gas wells

With the EUR prediction method of natural gas wells as a reference, previous EUR evaluation methods of shale gas wells have mostly comprised knowledge-driven methods. The knowledge-driven method, based on a relevant theoretical model or empirical equation of the target parameters to be calculated, involves the selection of required input parameters to perform calculations. EUR evaluation methods of shale gas wells mainly include the empirical production decline method, modern production decline method (including the flow material balance method), simulation prediction method (analytical model method and numerical simulation method) and probability method (Zhang et al., 2018, 2020; Zhao et al., 2019; Bi et al., 2020), as listed in Table 1. By means of analysis of these EUR evaluation methods of shale gas wells, the main factors influencing the EUR are determined.

The analytical model method, largely based on the simplified seepage mechanism under specific hypothetical conditions, establishes a gas seepage model of shale reservoirs to predict the EUR of shale gas wells. This method has mostly been applied in theoretical analysis and less in real production applications. However, by means of mathematical model integration by researchers, the relevant factors influencing the EUR of shale gas wells can be determined. The numerical simulation method, based on the simplified seepage mechanism mentioned above, implements the numerical method to fit production data and then predict the EUR. However, the numerical simulation method requires many parameters, and its application conditions are relatively limited.

The empirical production decline method includes the Arps empirical production decline method, Duong method, modified Duong method, power exponent decline method, modified power exponent decline analysis method and expanded exponent decline method. These methods are primarily based on the assumption of constant-pressure production but do not consider the complex seepage mechanism. Only a large number of production data is employed to analyze the EUR of shale gas wells, and this method has been widely applied. However, continuous production data of shale gas wells must be acquired, and the uncertainty is high for wells with less production data.

The material balance method, mainly based on the mass conservation law, captures the relationship among geological, recoverable and residual reserves and has been mostly applied to analyze

Table 1
Evaluation methods of the EUR of shale gas wells (adapted from Bi et al., 2020; Zhang et al., 2018; Zhang et al., 2020; Zhao et al., 2019).

EUR prediction method		Function	Applicable flow pattern	Applicable condition
Empirical production decline method	Arps decline method	Production/EUR prediction	Boundary-dominated flow	Constant-pressure production
	Expanded exponent decline method	Production/EUR prediction	Linear flow/boundary-dominated flow	Constant-pressure production
	Duong method	Production/EUR prediction	Linear flow section	Constant-pressure production
	Modified Duong method	Production/EUR prediction	Linear flow/boundary-dominated flow	Constant-pressure production
	Power exponent decline analysis method	Production/EUR prediction	Linear flow/boundary-dominated flow	Constant-pressure production
	Modified power exponent decline analysis method	Production/EUR prediction	Linear flow/boundary-dominated flow	Constant-pressure production
Modern production decline analysis method	Flow material balance method	EUR prediction	Boundary-dominated flow	Variable-pressure/rate production
	Fetkovich type curve method	EUR prediction	Boundary-dominated flow	Constant-pressure production
	Blasingame type curve method	EUR prediction	Transient flow/boundary-dominated flow	Variable-pressure/rate production
	Normalized pressure integral (NPI) type curve method	EUR prediction	Transient flow/boundary-dominated flow	Variable-pressure/rate production
	Agarwal-Gardner (A-G) type curve method	EUR prediction	Transient flow/boundary-dominated flow	Variable-pressure/rate production
	Wattenbarger method	EUR prediction	Transient flow/boundary-dominated flow	Variable-pressure/rate production
Simulation prediction method	Analytical method	Production/pressure/EUR prediction	All flow patterns	Variable-pressure/rate production
	Numerical simulation method	Production/pressure/EUR prediction	All flow patterns	Variable-pressure/rate production
Probabilistic method	Probabilistic cumulative production prediction method	EUR prediction	Transient flow/boundary-dominated flow	Variable-pressure production
	Phasic cumulative production prediction method	EUR prediction	Transient flow/boundary-dominated flow	Variable-pressure production

the relationship between gas production and formation pressure. The modern production decline method largely includes the Fetkovich type curve method, Blasingame type curve method and Wattenbarger method. The EUR of shale gas wells is evaluated based on the unsteady seepage theory and empirical methods, and this method is greatly influenced by artificial factors in the process of parameter or type curve matching, while numerous parameters are required.

The probabilistic method mainly includes the probabilistic cumulative production prediction method and probabilistic phasic production prediction method. This method comprehensively considers the uncertainty of the factors impacting the production of shale gas wells and emphasizes data uncertainty analysis to determine the EUR of shale gas wells based on data uncertainty factors, but the calculation method remains similar to the above methods. In the production practices of shale gas wells, each method requires specific application conditions. Hence, the uncertainty of EUR evaluation is high, and the selection of methods greatly impacts the EUR prediction of shale gas wells.

2.2. Deep feedforward neural network algorithm

Deep learning establishes complex expressions through other relatively simple expressions, namely, deep learning builds complex concepts based on relatively simple concepts, and the deep feedforward neural network is a typical deep learning model, as shown in Fig. 1. The deep feedforward neural network (DFNN) is a kind of artificial neural network, also called the feedforward neural network or multilayer perceptron. It is a typical deep learning algorithm model and better simulates and predicts the nonlinear relationship between input and output variables. From the mathematical perspective of the network model composition, the deep feedforward neural network with a nonlinear activation function

and a certain complexity can approach any continuous function, and it squares integrable functions with an arbitrary precision to accurately realize finite training sample sets (Hornik et al., 1989). Neurons are the most basic computing units of deep feedforward neural networks and are distributed in layers in the network. In each layer, the neurons are independent of each other and similar to multiple parallel operation units. They only receive information from the previous layer of neurons as input and then output information to the next layer of neurons. Because no information exchange occurs among neurons in the same layer and information is only transmitted forward in a stepwise manner, this method is called the deep feedforward neural network. The number of neuron distribution layers in the network determines the depth of the network, and the number of neurons in each layer determines the width of the network. Each neuron contains two parts: one part is the function composition model of the input part, which produces a weighted array of the information input received from the previous layer of neurons through weight allocation, and combined with the bias function, the function composition model is then formed; the other part is the activation function, mainly including the sigmoid function, tanh function, rectified linear unit (ReLU) function and Leaky-ReLU function (Eqs. (1)–(4)), which is applied to generate the nonlinear output of the function composition model.

In the 1980s–1990s, some basic ideas have appeared, like neural network back propagation algorithm, two-layer BP neural network, which is the basic model for convolutional neural network, recurrent neural network and feedforward neural network. Due to the computation limitation, these approaches have not yet been widely applied in practice. Until 2010, with the development of computation resources, deep learning has been better than traditional machine learning and artificial expert system in many fields. Since 2015, some mature deep learning networks have gradually developed, which has lowered the technical threshold for the
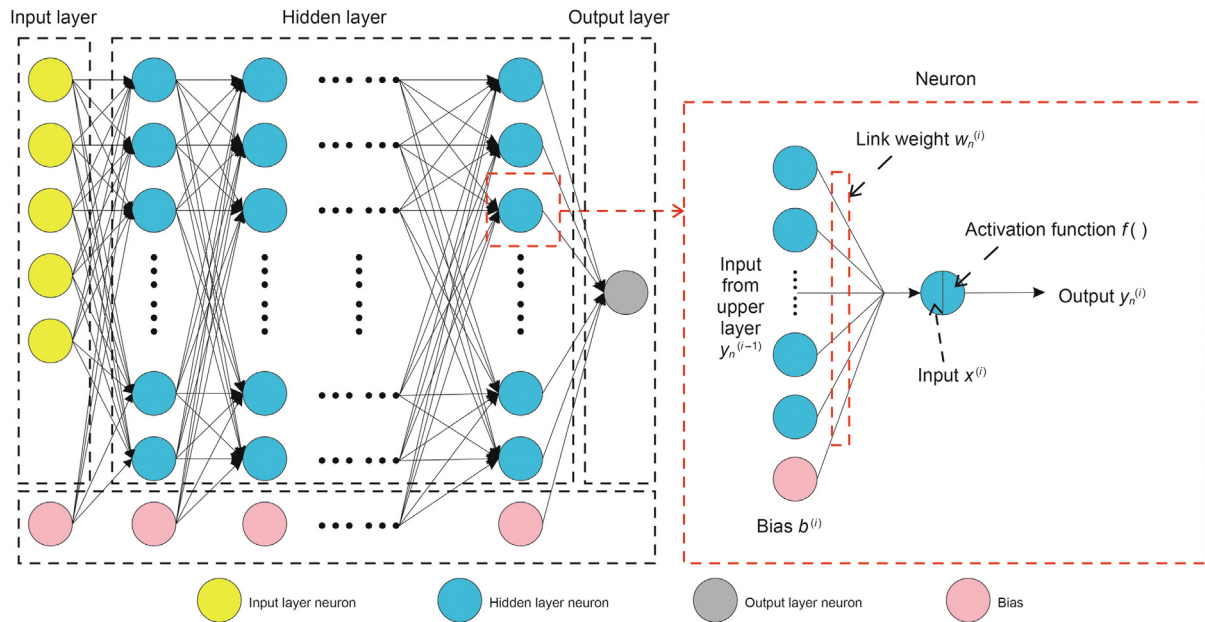
Fig. 1. Schematic diagram of the deep feedforward neural network (adapted from Liu, 2020).

popularization of deep learning methods in petroleum geology, and many scholars have begun to pay attention to this field. Since 2017, the related research results are no longer based on the application of traditional neural networks (BP networks). According to their characteristics and advantages, deep feed-forward network, convolutional neural network, recurrent neural network and generative adversarial network are gradually applied to the processing and interpretation of different areas in petroleum geology and engineering. Several researches have been operated in different shale reservoirs and different areas based on the DFNN. Production forecasting of Bakken Shale reservoirs is performed with high accuracy (Wang et al., 2019b). Traditional three layers neural network and DFNN is always applied in well logging prediction, interpretation, seismic interpretation and attributes prediction (David et al., 2018; Lu et al., 2021; Mattia, 2015; Shi et al., 2016). Although deep learning has made huge progress in petroleum related field, there are a lot of works need to be done to improve the accuracy and to explore the inner connection between different parameters.

Fig. 1 shows a typical network model of the deep feedforward neural network. The model contains three parts: input layer, hidden layer and output layer. The input and output layers generally contain only one layer, corresponding to the input and output data nodes, respectively. The hidden layer may contain multiple layers. Each neuron contains the output of the previous layer (which does not contain the input layer), the link weight, the bias function, the activation function and the output of the next layer (which does not contain the output layer); the output of the previous layer, the link weight and the bias function comprise the neuron input (Eq. (5)), while the activation function is implemented to nonlinearly output the above neuron input (Eq. (6)).

$$\text{sigmoid}(x) = \frac{1}{1 + e^{-x}} \tag{1}$$

$$\tanh(x) = \frac{e^x - e^{-x}}{e^x + e^{-x}} \tag{2}$$

$$\text{ReLU}(x) = \begin{cases} 0, & x < 0 \\ x, & x \geq 0 \end{cases} \tag{3}$$

$$\text{Leaky} - \text{ReLU}(x) = \begin{cases} \alpha \times x, & x < 0, \ 0 < \alpha < 1 \\ x, & x \geq 0 \end{cases} \tag{4}$$

$$x^{(i)} = \sum_{n=1}^{N} w_n^{(i)} y_n^{(i-1)} + b^{(i)} \tag{5}$$

$$y_n^{(i)} = f\left(x^{(i)}\right) \tag{6}$$

where $x^{(i)}$ is the input of the network neurons in the i layer; $w_n^{(i)}$ is the link weight of the $i-1$ layer output parameters at the time of input in the i layer; $y_n^{(i)}$ and $y_n^{(i-1)}$ are the output of the neurons in the i and $i-1$ layers, respectively; $b^{(i)}$ is the bias of the neurons in the i layer; N is the number of neurons in the previous layer connected to the neuron; and $f()$ is the activation function.

3. Method design

Based on the deep feedforward neural network, a deep learning-based EUR prediction method for shale gas wells is designed. As shown in Fig. 2, input data selection is performed first, data input is then performed based on the selected data. The input data are preprocessed to meet the demands of model training and prediction, and the data are divided into prediction and training data sets. Based on the training data set, the network model structure and parameters are defined. Subsequently, the network model is trained to meet the precision requirement, and finally, based on the prediction data set and the trained network model, EUR prediction of shale gas wells is carried out. The algorithm is realized by Python 3.7 and TensorFlow 1.15.

In the aspect of input data selection, a combination of knowledge- and data-driven modes is adopted, and the knowledge-driven mode is adopted as the basic and main mode, while the
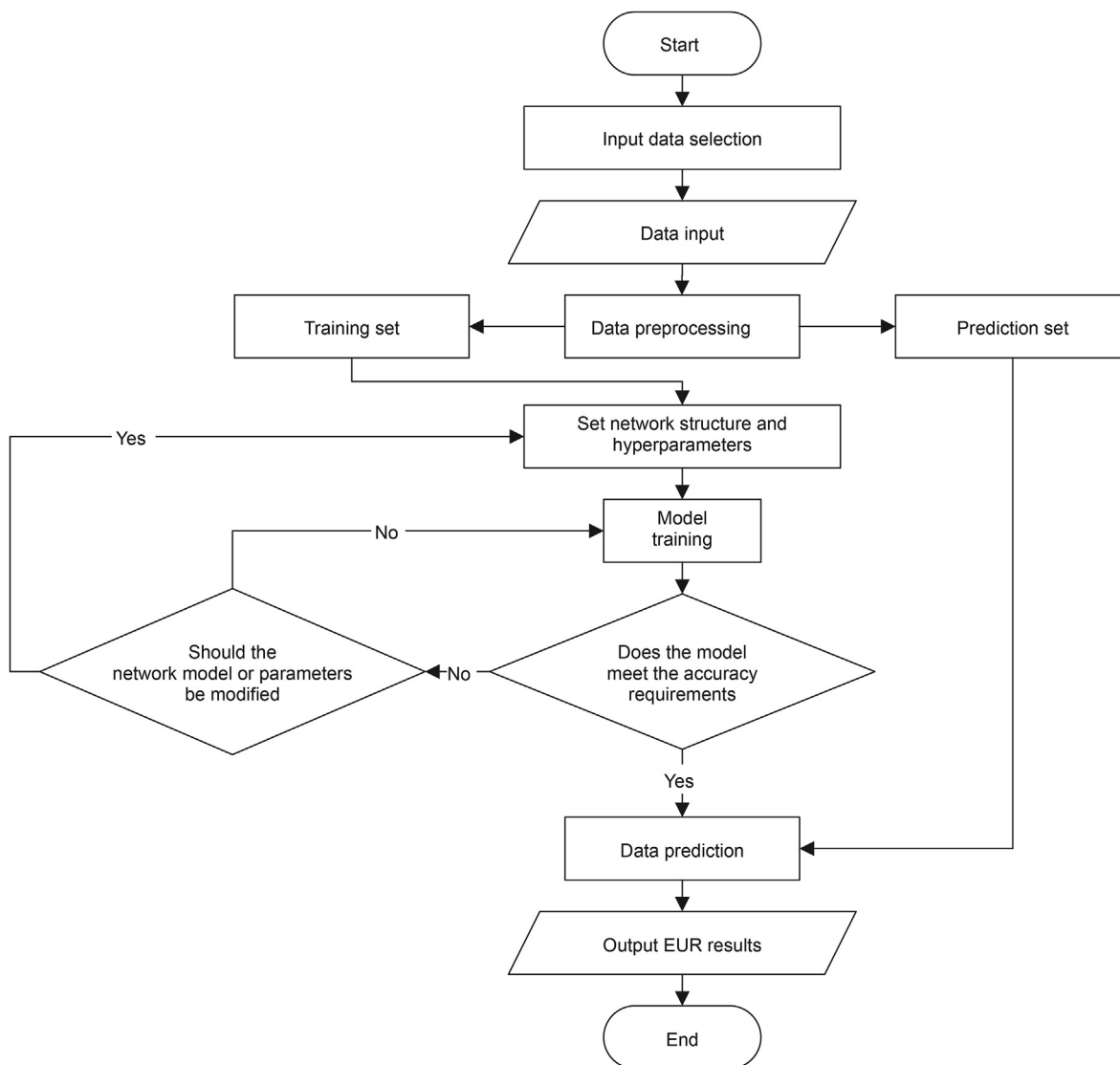
Fig. 2. Technical process of deep learning-based EUR prediction of shale gas wells.

data-driven mode is adopted as the auxiliary and supplementary mode. The knowledge-driven mode constitutes the basis: theoretical models generally establish relationships between input parameters and those in a target table in the ideal state from the perspective of the material composition and reservoir structure, thus reflecting the internal relation of objects. Empirical equations are commonly established in long-term scientific research and production practices, which statistically express the relationships between input parameters and those in a target table within a certain range. Therefore, the parameters used in these models and equations are usually strongly related to the target parameters and can be adopted as the main input parameters. The data-driven mode is supplementary: for specific data sets, on the one hand, a poor data quality of certain parameters may interfere with the deep learning model, and these interferences must be eliminated, while on the other hand, assessment of more parameters provides a better understanding of the selection of model input parameters. At the time of parameter selection, a variety of theoretical models and empirical equations to obtain the target parameters should be comprehensively considered, and relevant parameters should be selected as input to reconstruct the relationship between them and

target parameters through deep learning.

In the aspect of data preprocessing, the selected input data should be systematically processed. Before training, all input parameters must be standardized to eliminate any differences in the order of magnitude between the various input parameters and prevent certain parameters from dominating due to their order of magnitude, which further affects training and prediction. Based on the function of data sets, the data samples are divided into training and prediction data sets according to a certain proportion through random sampling. The training data set is primarily used to train the neural network model, and the prediction data set comprises the main data for EUR prediction.

The objective of setting the network model structure and parameters is to obtain a suitable rather than optimal network structure and parameter combination, and the standard of the former is based on the actual application requirements. In particular, the model size is related to the task objective and the size of the data set. The EUR prediction of shale gas wells is influenced by factors such as geological factors, engineering factors, production systems, data acquisition modes and raw data processing modes and exhibits an obvious regionality. The establishment of data sets

is only based on one area and one place. Compared to the existing data sets analyzed for image and natural language processing purposes, a large gap in quantity and quality occurs. Therefore, the direct use of network structures commonly applied in these fields easily leads to high training costs and unsatisfactory learning effects, and networks of an appropriate size should be designed according to different application scenarios.

Model training requires a certain number of trials and errors to obtain a suitable model that meets the demand of the application. On the one hand, randomness occurs in the initialization process of the deep learning network. On the other hand, it is necessary to determine suitable model types, input data and parameter combinations. At the time of prediction, the input parameters are entered into the network to obtain the EUR of target shale gas wells.

4. Application test

4.1. Introduction of the regional basic situation

The WY shale gas field is located in the south of the Sichuan Basin, China, with an area of approximately 4204 km². To the north, a mountainous landform is present, and most of the central areas to the south are hilly landforms. The terrain is tilted from northwest to southeast, while both low mountains and hills occur, and the elevation ranges from 300 to 800 m. Tectonically, the WY shale gas field belongs to the low fold belt in the paleoslope of southwestern Sichuan Province, where the Weiyuan anticline is developed, Triassic and Jurassic formations crop out, Devonian and Carboniferous formations are absent vertically, and Silurian formations are missing to varying degrees in the northwest of the anticline. The burial depth of the bottom of the Wufeng Formation, the Longmaxi Formation, of the WY shale gas field ranges from 1500 to 4000 m, strata suffer from different degrees of denudation in the northwest, and the burial depth increases from northwest to southeast.

The target horizon of the WY shale gas field in the study area is the Longmaxi Formation, specifically, the Long 1_1 sublayer. The organic matter abundance of this interval is high as a whole, with a measured total organic carbon (TOC) content of 0.1%–8.2% (2.9% on average), and the TOC value got by well logs is between 1.3% and 7.7% (3.6% on average). The porosity is high and relatively stable, with a measured porosity of 2.0%–7.4% (5.4% on average) and porosity got by well logs is between 3.5% and 9.1% (6.1% on average). The gas saturation is relatively high, with a measured gas saturation of 32.7%–84.6% (64.7% on average) and gas saturation got by well logs is between 5.3% and 74.7% (53.6% on average). The measured gas content ranges from 0.9 to 11.4 m³/t (4.3 m³/t on average), and gas content got by well logs is between 2.6 and 8.7 m³/t (5.7 m³/t on average). The measured brittle mineral content is relatively high as a whole, from 50.0% to 95.6% (72.1% on average), and the brittle mineral content got by well logs is between 58.0% and 88.3% (70.7% on average). The distribution of the ground stress is highly uneven, with the maximum principal stress ranging from 70.00 to 89.50 MPa (80.71 MPa on average), and the minimum principal stress ranging from 54.00 to 80.00 MPa (68.66 MPa on average). The horizontal stress difference varies greatly and ranges from 7.65 to 18.70 MPa. The direction of the maximum horizontal principal stress changes little and basically remains the same, nearly east-west, between NE70° and NE130° (approximately 90° on average). The preservation conditions of the shale gas reservoir are good, with the formation temperature varying from 71.80 to 133.92 °C and the formation pressure varying from 13.79 to 73.31 MPa, while the pressure coefficient ranges from 0.92 to 1.99. As of October 2020, a total of 419 wells has been drilled in the WY shale gas field, among which 282 wells have EUR evaluation data. According to real production data, the above wells all adopt natural production, without pressure control, pressure channeling and other special circumstances, and no well stimulation measures such as artificial lift have been applied.

4.2. Data dependency analysis

Data dependency analysis was conducted on the basis of the 282 shale gas wells with EUR evaluation data in the region, mainly including 17 influencing parameters such as geological factors (TOC, porosity, high-quality reservoir thickness, gas saturation, pressure coefficient, and brittle mineral content), engineering factors (fracturing section length, number of fracturing sections, true vertical depth, average section spacing, liquid strength, sanding strength, average displacement, drilling length of high-quality reservoirs, and drilling length of the target layer) and production factors (test output and first-year daily gas flow rate), as listed in Table 2.

The high-quality reservoir thickness and drilling length of high-quality reservoirs are all related to high-quality reservoirs. Based on the actual production situation in the test area, high-quality reservoirs mainly exhibit a high TOC content (>4%), high porosity (>6%), high gas saturation (>70%) and high brittle mineral content (>75%) (Ma et al., 2020a, 2020b). The target layer largely refers to the Long 1_1 sublayer of the Longmaxi Formation. The drilling length of high-quality reservoirs mostly refers to the distribution area of high-quality shales in the drilling length of the target layer, so in general, the drilling length of high-quality reservoirs is smaller than or equal to the drilling length of the target layer.

The factor correlation was analyzed based on the above 17 factors and EUR evaluation results. The data dependency was determined by the correlation coefficient between factors (Eq. (7)), with the results listed in Table 3. When a strong correlation occurs between factors at a correlation coefficient greater than 85%, the test output and daily gas flow rate (0.98), the true vertical depth and pressure coefficient (0.87), the test output and EUR (0.94) and the daily gas flow rate and EUR (0.96) exhibit notable correlation relationships.

Overall, the EUR demonstrates a strong correlation with multiple parameters. In particular, 9 factors such as the fracturing section length (0.54), number of fracturing sections (0.45), test output (0.94), first-year daily gas flow rate (0.96), high-quality reservoir thickness (0.35), gas saturation (0.41), brittle mineral content (0.41), drilling length of high-quality reservoirs (0.50) and drilling length of the target layer (0.49) exhibit a very strong dependency on the EUR, while 8 factors such as the true vertical depth (−0.11), TOC (−0.17), porosity (−0.05), pressure coefficient (−0.02), average section spacing (−0.06), liquid strength (0.03), sanding strength (0.18) and average displacement (0.08) do not exhibit an obvious dependency on the EUR, which basically agrees with the findings of other researchers (Ma et al., 2020a, 2020b).

$$r(x, y) = \frac{Cov(x, y)}{\sqrt{S(x) \cdot S(y)}} \tag{7}$$

where $r(x, y)$ is the correlation coefficient between variables x and y; $Cov(x, y)$ is the covariance between variables x and y; and $S(x)$, $S(y)$ are the variance in variables x and y, respectively.

Normalization processing (Eq. (8)) was conducted for each influencing factor to eliminate any differences in the order of magnitude among the various input parameters, the results box chart and distribution histogram is listed in Figs. 3 and 4, and linear dependence analysis of the data was then conducted, while the correlation between EUR and aforementioned parameters was determined after normalization. Fig. 5 shows the correlation analysis results between the geological factors and EUR, Fig. 6 shows

Table 2
Statistics of the data.

Data type	Unit	Data size	Mean	Standard deviation	Maximum	Minimum
Fracturing section length	m	281	1515.87	308.47	2577.00	502.00
Number of fracturing sections	Dimensionless	281	22.63	5.56	36.00	3.00
Test Production	10^4 m^3/d	281	20.94	12.10	78.08	1.81
First-year average daily gas production	10^4 m^3/d	281	9.47	5.28	34.02	0.98
True vertical depth	m	279	3008.24	352.49	3800.00	2200.00
TOC	%	282	5.39	0.76	7.80	3.30
Porosity	%	282	7.11	0.96	8.90	5.00
High-quality reservoir thickness	m	282	5.17	1.36	7.50	2.30
Gas saturation	%	279	75.70	3.14	83.00	60.00
Pressure coefficient	Dimensionless	282	1.74	0.19	2.05	1.35
Brittle mineral content	%	282	78.67	7.79	96.00	62.50
Average section spacing	m	281	69.94	27.81	479.33	43.10
Liquid strength	m^3/m	281	27.25	4.51	47.94	7.12
Sanding strength	t/m	281	1.63	0.38	3.00	0.29
Average displacement	m^3/min	281	11.80	1.33	15.00	6.19
Drilling length of high-quality reservoirs	m	208	1002.24	460.57	2380.50	0.00
Drilling length of the target layer	m	195	1349.79	443.87	2315.50	0.00
EUR	10^8 m^3	282	0.89	0.43	2.65	0.12

Table 3
Correlation coefficient between the main factors and EUR.

Data type	Correlation coefficient with the EUR	Data type	Correlation coefficient with the EUR
Fracturing section length	0.54	True vertical depth	−0.11
Number of fracturing sections	0.45	TOC	−0.17
Test output	0.94	Porosity	−0.05
First-year daily gas flow rate	0.96	Pressure coefficient	−0.02
High-quality reservoir thickness	0.35	Average section spacing	−0.06
Gas saturation	0.41	Liquid strength	0.03
Brittle mineral content	0.41	Sanding strength	0.18
Drilling length of high-quality reservoirs	0.5	Average displacement	0.08
Drilling length of the target layer	0.49		

the correlation analysis results between the production factors and EUR, Fig. 7 shows the correlation analysis results between the engineering factors and EUR, and the linear dependence analysis results between the main factors and EUR are listed in Table 4.

$$\begin{cases} x_n = \dfrac{x - \mu(x)}{\sigma(x)} \\ \mu(x) = \dfrac{1}{N}\sum_{i=1}^{N} x_i \\ \sigma(x) = \sqrt{\dfrac{1}{N}\sum_{i=1}^{N}(x_i - \mu(x))} \end{cases} \tag{8}$$

where x, x_n are factor variables before and after normalization; $\mu(x)$ is the expectation of variable x; $\sigma(x)$ is the standard deviation of variable x; and N is the number of sample points of variable x.

The above results indicate that among the geological, engineering, and production factors, parameters such as the test output (0.9300) and first-year daily gas flow rate (0.8907) exhibit a more obvious linear relation with the EUR, while other parameters do not exhibit an obvious linear dependence on the EUR of shale gas wells. Therefore, a nonlinear relation between the various influencing factors and EUR is effectively captured by the adopted deep learning algorithm.

4.3. Deep feedforward neural network-based EUR prediction

Based on the data size and data dependency analysis results, selecting the EUR as the final evaluation target, 6 different data combinations were designed as input data for network training and prediction purposes. The specific network training data combinations are as follows (Table 5): (1) high-correlation parameter combination: fracturing section length, number of fracturing sections, test output, first-year daily gas flow rate, high-quality reservoir thickness, gas saturation, brittle mineral content, drilling length of high-quality reservoirs and drilling length of the target layer; (2) low-correlation parameter combination: true vertical depth, TOC, porosity, pressure coefficient, average section spacing, liquid strength, sanding strength and average displacement; (3) full parameter combination: contains 17 parameters; (4) combination of high- and low-correlation mixed samples and the largest amount of sample data: all parameters except the drilling length of the target layer and high-quality reservoir; (5) combination of high- and low-correlation mixed samples, with the same number of input samples as case 3 including static parameters: all parameters except production factors (test output and first-year daily gas flow rate), i.e., combination of static geological and engineering parameters; and (6) all parameters except the drilling length of high-quality reservoirs.

For the deep feedforward network, the design of the network structure and hyperparameters must consider the size of the data set to balance the learning ability, training efficiency and training difficulty of the model. A deeper network provides a stronger learning ability, but this does not greatly improve the effect. After testing, a deep feedforward neural network with an 8-layer structure exhibits obvious advantages in regard to the accuracy and training efficiency of the EUR prediction network model. Therefore, the network is set to 8 layers, and the network structure is X (the number of neuron nodes in the input layer determined based on the number of input parameters, namely, 9 in case 1, 8 in case 2, 17
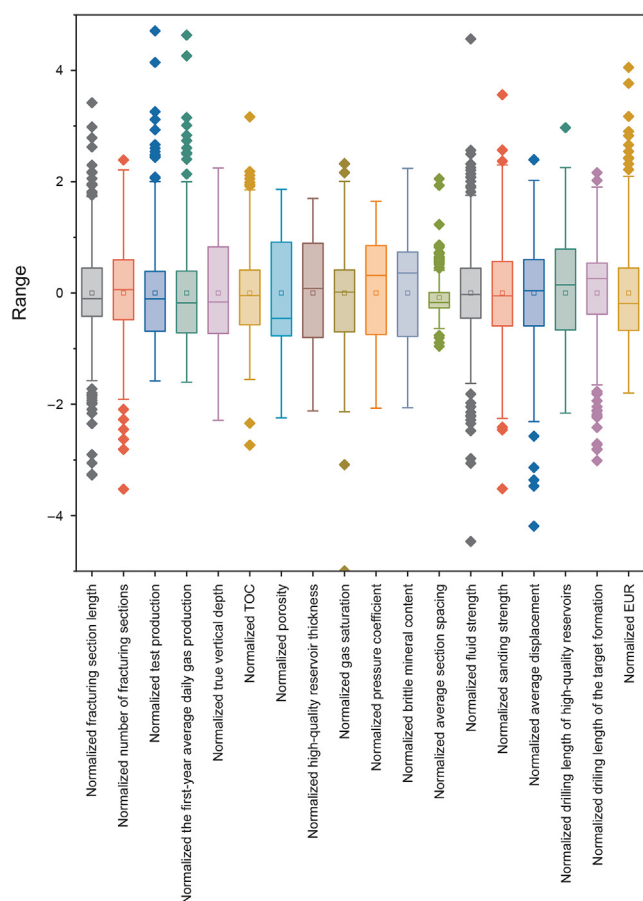
Fig. 3. Box chart of the WY shale field normalized data.

deep learning model of this paper, the Leaky-ReLU function (Eq. (4)) is mainly adopted as the activation function, in which $\alpha = 0.2$.

Deep learning adopts the loss function as the optimization objective and adjusts model parameters to obtain a set of parameters ensuring that the model output value approaches the actual value. The optimization parameters are used to control the process of model parameter adjustment, which exerts a direct impact on the training efficiency and learning effect of the model. The learning rate is one of the parameters that are difficult to set (Goodfellow et al., 2016), and it notably impacts the network performance. If the learning rate is too low, training convergence occurs very slowly, and if the learning rate is too high, this may also hinder convergence and cause the loss function to fluctuate near its minimum value. Therefore, an adaptive learning rate method is proposed. Hinton and his colleagues developed the RMSProp learning rate adjustment method (Hinton et al., 2006; Hinton and Salakhutdinov 2006; Tieleman and Hinton, 2012), which is automatically adjusted based on the model scale and greatly facilitates the learning rate parameter setting process. Hence, the learning rate adjustment method adopted in this paper is RMSProp. What's more, the initializer algorithm is glorot_uniform, the regulate parameter is 0.3 and the moving average decay is 0.9.

Normalized processing was performed for all data based on the data composition of the different test cases. A ratio of 3:1 of the training set to the test set was adopted, and the training and prediction sets were divided by random sampling, after which network training and prediction were performed. First, the deep neural network was trained based on the training data set. Second, with the help of the trained deep neural network model, combined with the prediction data set, prediction of the normalized EUR of shale gas wells was conducted. Third, with Eq. (8), inverse normalization was carried out of the prediction results to obtain the EUR prediction results of wells. Finally, the EUR prediction results of wells were compared to the actual EUR results. In regard to the test results of each case, the average relative error, absolute value of the average relative error and root mean square error between the true values of the training and prediction sets of each case and the model prediction values were calculated, with the evaluation results summarized in Table 6 and shown in Fig. 8.

4.4. Results and discussion

The above results reveal that network prediction and simulation based on the high-correlation parameters of the EUR (case 1) greatly reduce the error of the prediction results, and the error of the training set is controlled within 5%, while the data accuracy of the prediction set is high, within 15%. Moreover, the data deviation degree is also very low. However, compared to the other cases, e.g., cases 3 to 6, the input data and data size of the high-correlation factors are relatively small, which imposes a certain impact on the training and prediction stages of the model and thus affects the EUR evaluation results. The data size of the low-correlation parameters (case 2) is obviously large, but the EUR prediction results are generally poor, the relative error is large, and the data deviation degree is obviously high. However, the prediction results demonstrate that the low-correlation parameters also yield a certain data pattern and a certain control effect on the EUR.

After comprehensively considering the effect of the data correlation degree and data size, the high- and low-correlation parameters were integrated to perform EUR prediction (case 3). Although the data size was reduced to a certain extent, the results of the training and prediction sets had been obviously improved over the previous results, and the data deviation degree notably decreased. The above results further show that under certain conditions, the low-correlation data also impose a certain impact on the EUR prediction results. In terms of the EUR prediction results controlled
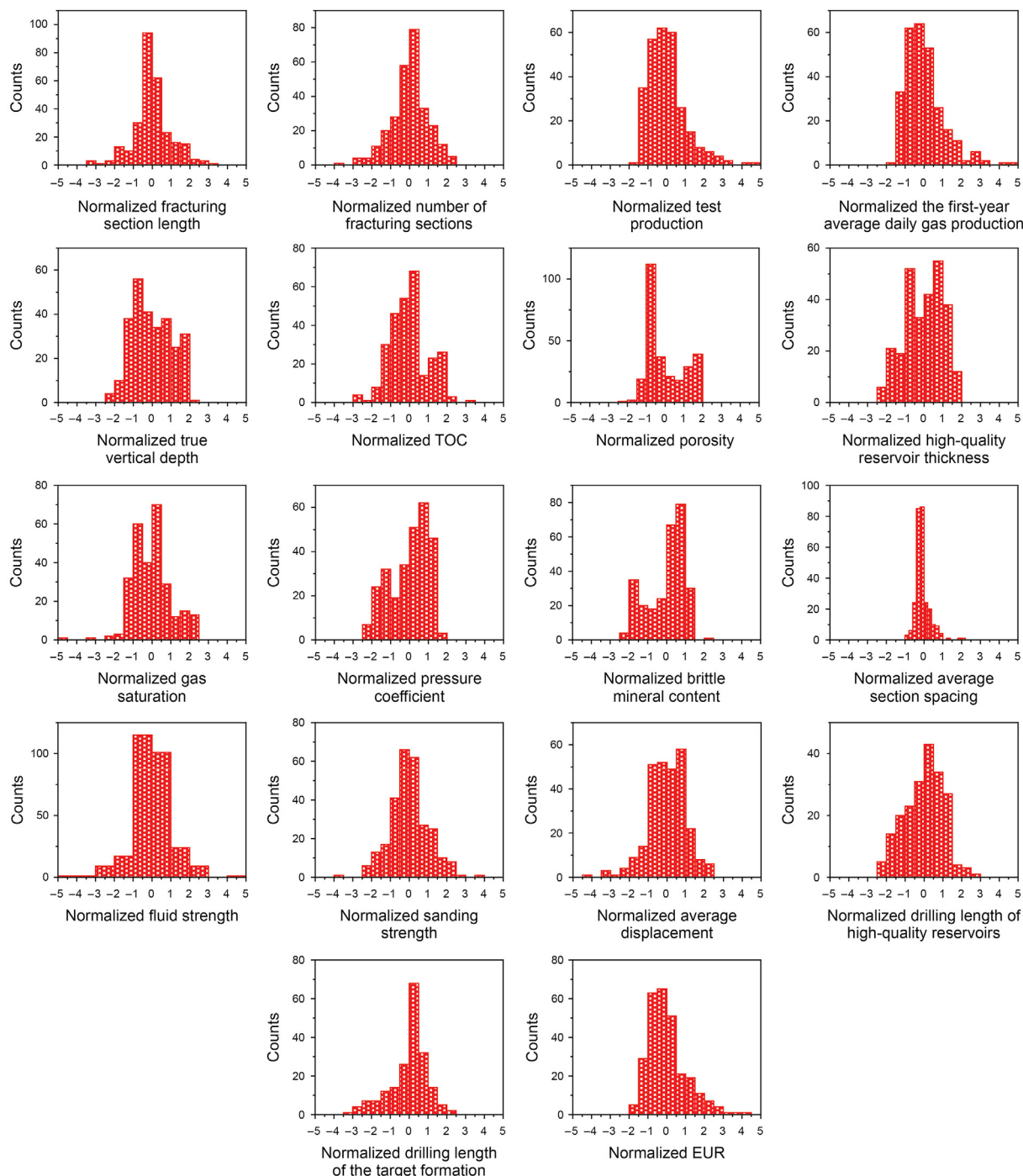
in case 3, 15 in cases 4 and 5, and 16 in case 6)-50-40-30-20-10-5-1 (the grid node of the output layer, i.e., the normalized EUR of shale gas wells).

The activation function is applied to achieve nonlinear mapping between the input and output, and its derivative is propagated at the time of back propagation and optimization of the network parameters. Therefore, the properties of the activation function and its derivative impose an important influence on the application effect of the deep learning model. The sigmoid and tan activation functions are commonly applied in traditional neural networks, but in the process of back propagation in deep model training, the derivatives are smaller than 1 and rapidly decrease at positions deviating from 0. After multiple product calculations, the gradient readily disappears. The derivative of the ReLU function (Eq. (3)) which has attained a breakthrough in deep learning at the early stage, is identically equal to 1 when the x value is greater than 0, and this solves the problem of gradient disappearance to a certain extent (Krizhevsky et al., 2012). However, when the x value is less than 0, the activation function and its derivative value are all 0, which results in invalid neurons, thus leading to an unstable model training process, and the final training effect is impacted. To allow the activation function to better meet the training needs of the deep network, the ReLU function has been improved by processing the function form at a x value less than 0. Among the improved ReLU functions, the Leaky-ReLU function (Eq. (4)) is one of the most commonly used activation functions. When the x value is less than 0, the derivative of the activation function is identically equal to a coefficient greater than 0, which solves the problem occurring in traditional activation functions (Maas et al., 2013). Therefore, in the

Fig. 4. Distribution histogram of the WY shale field normalized data.

by multiple parameters, even if the data dependency is unclear, good EUR prediction results could be obtained by prediction and evaluation based on integrated parameters.

In the case whereby the sample size of the high- and low-correlation comprehensive parameter evaluation data is small, parameter combination under the condition of maximum data samples (case 4) was applied to predict the EUR. The data sample size in case 4 was 45.7% larger than that in case 3, but the parameter combination did not contain the drilling length of high-quality reservoirs and drilling length of the target layer with a high correlation (the effective data points of these two factors were

relatively scarce). The data sample size in case 4 was the same as that in case 2, but high-correlation input parameters were included. Compared to case 2, the training and prediction effects were greatly improved, and the relative error and root mean square error were notably reduced, showing that the number and correlation of input parameters greatly influence the EUR prediction results. However, compared to case 3, although the sample size had largely increased, shortcomings remained in regard to the training and prediction effects due to the lack of the above two high-correlation influencing factors, further indicating that the data dependency also exerts a certain impact on the EUR prediction results. The relationship
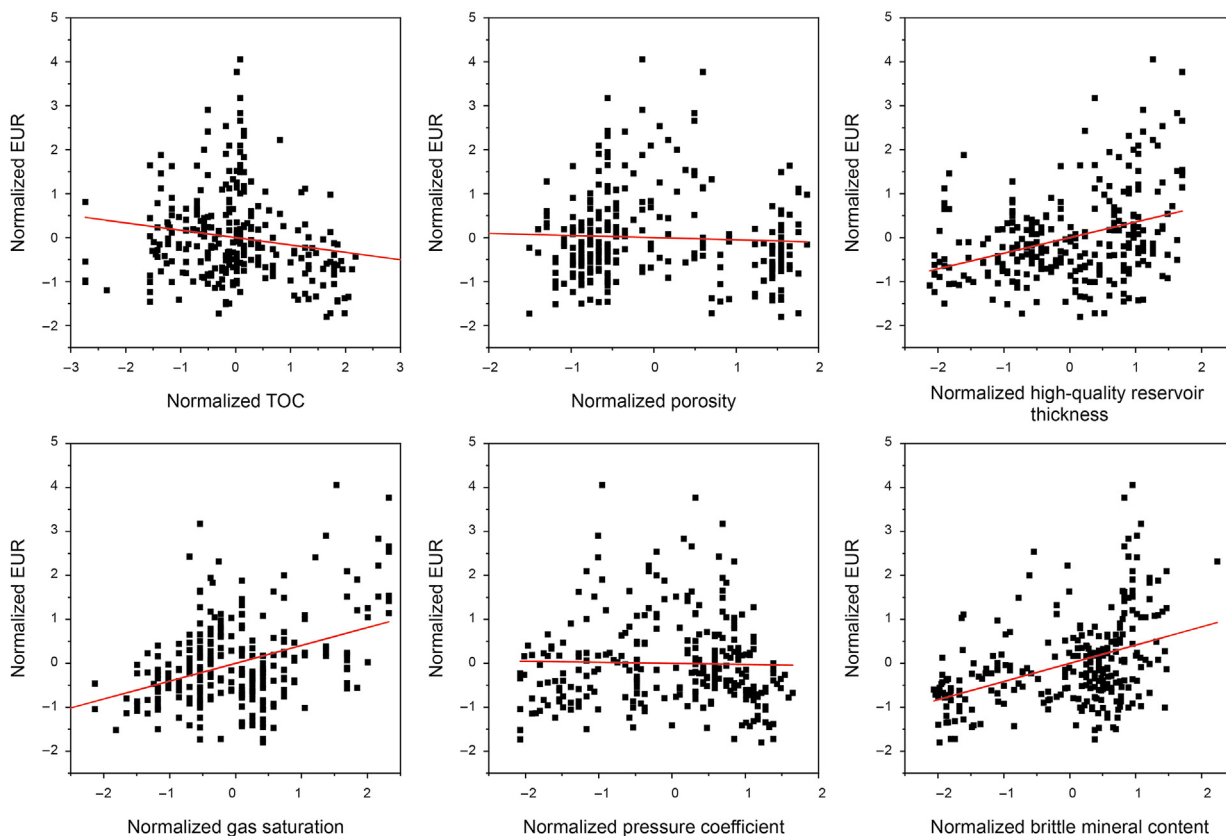
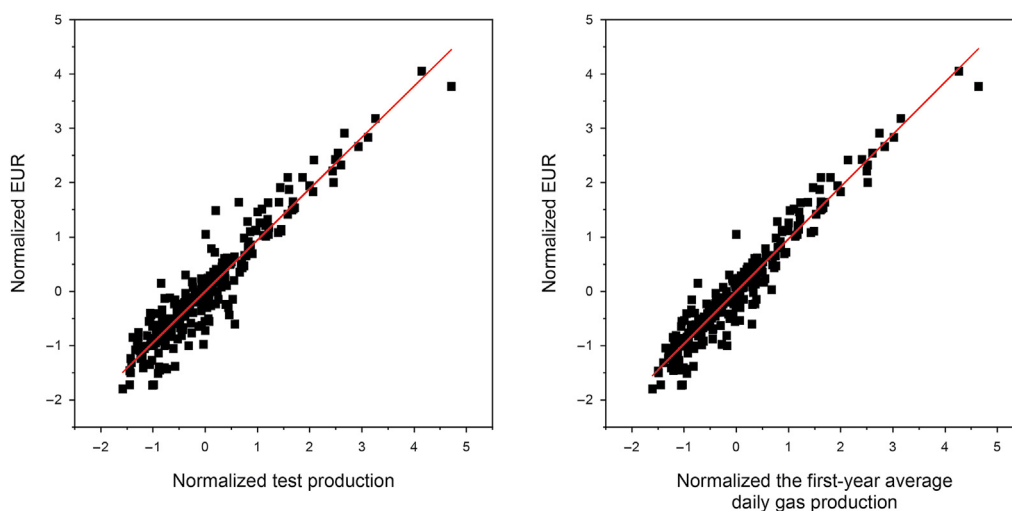Fig. 5. Linear dependence analysis of the normalized geological factors and EUR.

Fig. 6. Linear dependence analysis of the normalized production factors and EUR.

between the above two high-correlation factors and EUR is also consistent with the research results of other researchers (Ma et al., 2020a, 2020b).

A test was carried out in case 5 by removing 2 high-correlation production factors while maintaining the same data sample size as that in case 3. Compared to cases 2 and 4, the data size was also reduced to a certain extent. The test results demonstrate that the accuracy of the training and prediction sets was still relatively low, and the data deviation degree remained lower than that of the low-correlation sample combination of case 2. In the case of fewer input parameters, the correlation between the considered factors and EUR imposes a major effect on the prediction results. It is expected that the prediction effect may also be further improved by increasing the sample size. Overall, the effect of factor correlation on the prediction results is obviously greater than that of the data sample size. Moreover, case 5 also further revealed that in the case when production factors are unavailable, only through the combination of static geological parameters and engineering parameters
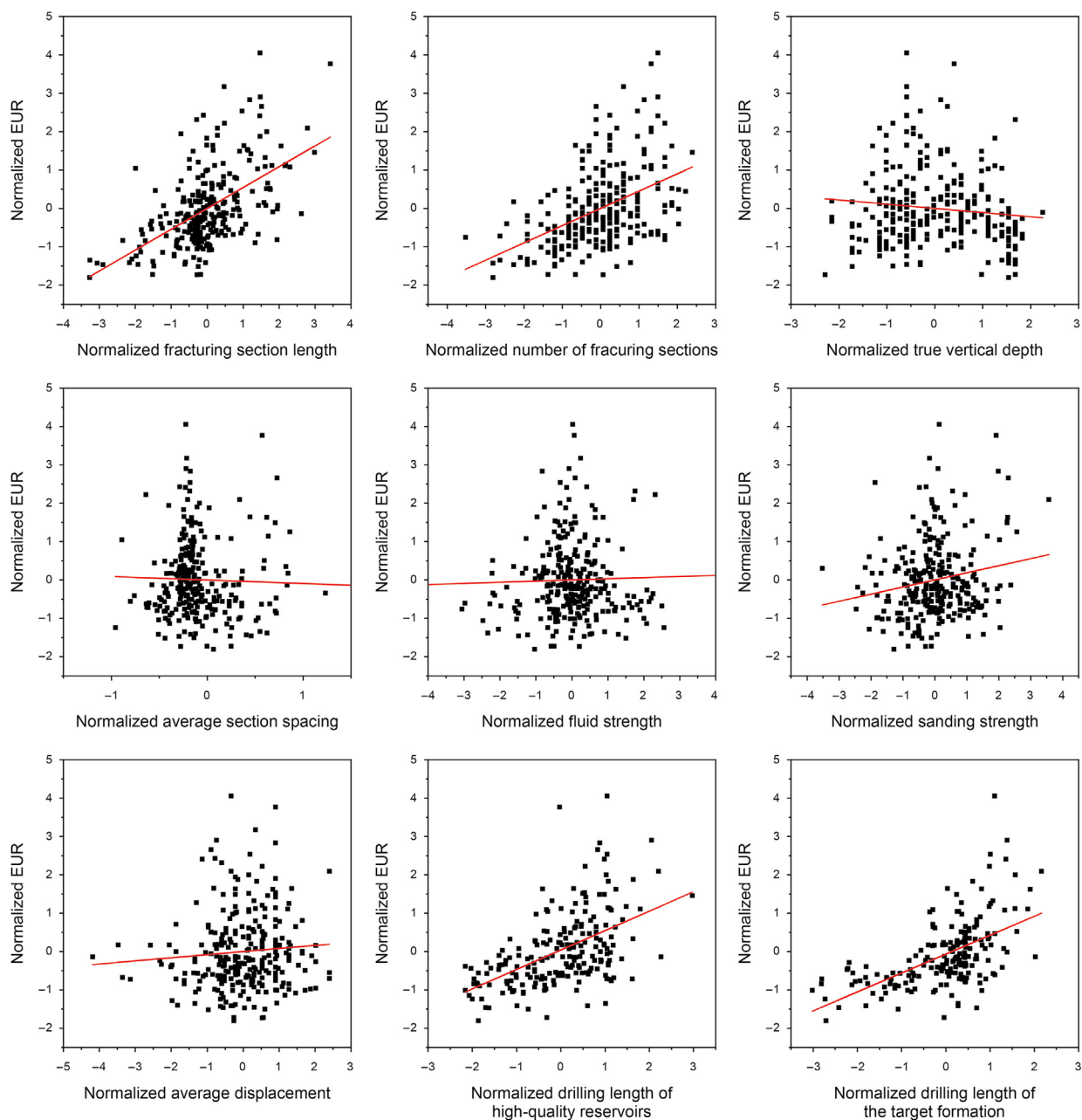
Fig. 7. Linear dependence analysis of the normalized engineering factors and EUR.

Table 4
Linear dependence analysis results of the main factors and EUR data.

Data type	Linear correlation coefficient	Data type	Linear correlation coefficient
Fracturing section length	0.2961	TOC	0.0281
Number of fracturing sections	0.2025	Porosity	0.0025
True vertical depth	0.0119	High-quality reservoir thickness	0.1263
Average section spacing	0.0011	Gas saturation	0.1655
Liquid strength	0.0009	Pressure coefficient	0.0006
Sanding strength	0.0345	Brittle mineral content	0.1716
Average displacement	0.0066	Test output	0.9300
Drilling length of high-quality reservoirs	0.2665	First-year daily gas flow rate	0.8907
Drilling length of the target layer	0.3130		

may the method proposed in this paper be applied to predict the EUR of shale gas wells, and the prediction results also exhibit a certain accuracy.

A test was carried out in case 6 by removing the drilling length

Table 5
Classification of the network training parameters.

Data type	Case 1	Case 2	Case 3	Case 4	Case 5	Case 6
Fracturing section length	✓	–	✓	✓	✓	✓
Number of fracturing sections	✓	–	✓	✓	✓	✓
Test output	✓	–	✓	✓	–	✓
First-year daily gas flow rate	✓	–	✓	✓	–	✓
True vertical depth	–	✓	✓	✓	✓	✓
TOC	–	✓	✓	✓	✓	✓
Porosity	–	✓	✓	✓	✓	✓
High-quality reservoir thickness	✓	–	✓	✓	✓	✓
Gas saturation	✓	–	✓	✓	✓	✓
Pressure coefficient	–	✓	✓	✓	✓	✓
Brittle mineral content	✓	–	✓	✓	✓	✓
Average section spacing	–	✓	✓	✓	✓	✓
Liquid strength	–	✓	✓	✓	✓	✓
Sanding strength	–	✓	✓	✓	✓	✓
Average displacement	–	✓	✓	✓	✓	✓
Drilling length of high-quality reservoirs	✓	–	✓	–	✓	–
Drilling length of the target layer	✓	–	✓	–	✓	✓

Note: the '√' means that this factor is included in the network input data and '-' refers to the opposite.

Table 6
Network training and prediction results.

	Case 1	Case 2	Case 3	Case 4	Case 5	Case 6
Data sample size	192	274	188	274	188	201
Sample size of the training set	134	206	141	206	141	151
Sample size of the prediction set	48	68	47	68	47	50
Average relative error of the training set, %	0.97	4.85	1.19	1.89	−2.52	−1.29
Average relative error of the prediction set, %	−3.81	14.41	7.07	−2.88	10.07	−0.68
Absolute value of the average relative error of the training set, %	4.63	14.41	3.79	4.42	10.60	4.48
Absolute value of the average relative error of the prediction set, %	13.58	48.33	12.81	13.53	16.60	5.02
Root mean square error of the training set	0.06	0.25	0.07	0.06	0.23	0.05
Root mean square error of the prediction set	0.14	0.50	0.14	0.13	0.21	0.07

of high-quality reservoirs with few data points and a high correlation degree, but the types of neural network input samples increased over cases 4 and 5 (16 input samples in case 6 and 15 input samples in cases 4 and 5). Although the data sample size was not large, the data accuracy had been obviously improved, and the data deviation degree was also relatively low. The above results show that the high-correlation factors of the EUR, such as the drilling length of the target layer, greatly contribute to the accuracy of the EUR prediction results of shale gas wells.

In summary, the EUR prediction model of shale gas wells in this area has basically been built based on the deep neural network, the feasibility of the method proposed in this paper has been effectively demonstrated, a good effect has been attained through regional data testing, and the accuracy of the method has been verified. However, certain constraints may still remain in the application and popularization of the EUR prediction model of shale gas wells established using the above method in other areas, i.e., the model applicability must be further investigated. The results of WY shale gas well EUR prediction is good, for the other areas, the same kind of data need to be collected and the network hyperparameters should be adjusted. For the current training model, some new parameters of other areas should be added to enrich this model and extended to some new area. On the hand, the data using in this manuscript, mainly including the data variety, needed to be collected and the hyperparameters should be adjust to train a new network for another area following the procedure proposed in this manuscript. Thus, this method needs a large number of data group. On the other hand, when we deal with some area which is similar to the situation of WY area, we only using a small group data to retrain this model and using the same network can perform it to another area. The number of shale gas wells in the area continuously

increases, and the EUR evaluation results and influencing factor data are continuously enriched, which are of great significance to the further improvement of the deep learning EUR prediction model for this area. Moreover, based on the training and prediction results of the deep neural network, the data size (including the number of input parameters, the method of data combination and the number of data sample points) also exerts a certain impact on the training and prediction results of the model. Detailed analysis and demonstration should be further performed regarding the specific influence to provide a certain theoretical support.

5. Conclusions

This paper systematically analyzes the existing EUR evaluation methods of shale gas wells, describes the basic connotation of the deep learning algorithm, introduces the deep learning algorithm in the EUR evaluation process of shale gas wells, establishes a deep feedforward neural network-based EUR evaluation method of shale gas wells, and analyzes actual data acquired from 282 wells in the WY shale gas field to test the validity of the method. The prediction results demonstrate a good consistency with the actual results, and the error is small. The following main conclusions are drawn:

(1) This paper first systematically analyzes the existing EUR evaluation methods of shale gas wells and the deep learning algorithm and then designs a deep feedforward neural network-based EUR evaluation method of shale gas wells. By integrating geological factors, engineering factors and production factors, this method quickly and effectively predicts the EUR of shale gas wells based on relevant basic parameters, and the prediction results exhibit a high accuracy.
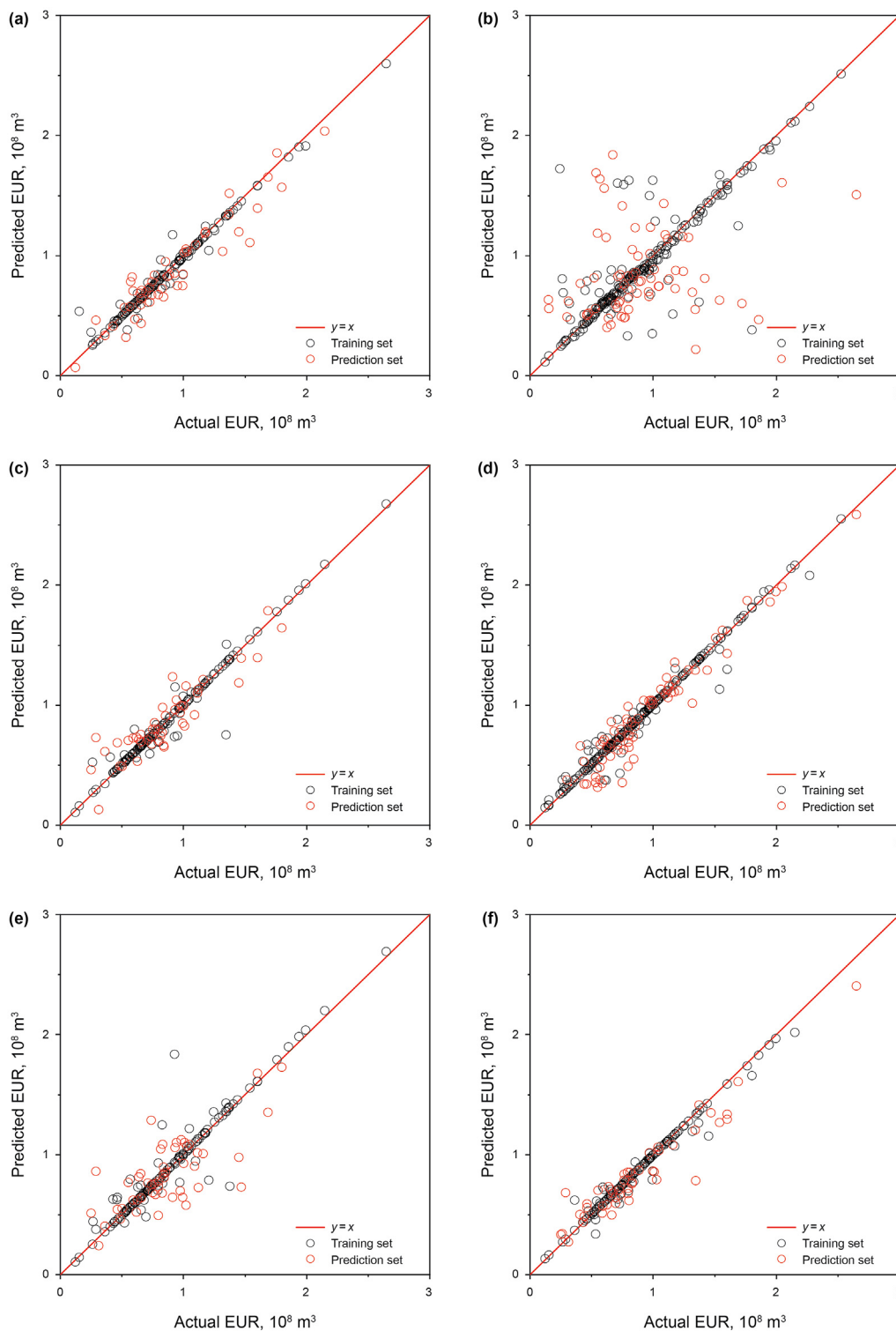
Fig. 8. Predicted vs actual EUR: (**a**) Case 1; (**b**) Case 2; (**c**) Case 3; (**d**) Case 4; (**e**) Case 5; (**f**) Case 6.

(2) On the basis of 282 shale gas wells with EUR evaluation results in the WY area, this paper performs data dependency analysis on 17 parameters of the geological, engineering and production factors involved in the EUR prediction method of shale gas wells. The analysis results show that the EUR exhibits a strong correlation with multiple parameters, such as the fracturing section length, but exhibits no obvious

correlation with various other parameters, such as the true vertical depth. Nine factors, such as the fracturing section length, number of fracturing sections, test output, first-year daily gas flow rate, high-quality reservoir thickness, gas saturation, brittle mineral content, drilling length of high-quality reservoirs and drilling length of the target layer, reveal a very high data dependency on the EUR. Eight factors,

including the true vertical depth, TOC, porosity, pressure coefficient, average section spacing, liquid strength, sanding strength and average displacement, reveal no obvious data dependency on the EUR.

(3) In regard to the 282 shale gas wells in the WY area, based on correlation analysis of the influencing factors, 6 different test cases are designed to test the EUR prediction method of shale gas wells proposed in this paper. The test results demonstrate that the proposed method could be used to effectively build an EUR prediction model of the shale gas wells in the study area. The type of input data and the correlation between the input data and prediction results (EUR) are the main controlling factors of the model accuracy, and the data size (including the number of input data and the data sample size) also exerts a certain impact on the model accuracy. This paper preliminarily analyzes the influence of hyperparameters such as the activation function and loss function on the method. In subsequent studies, the influence of the general applicability of the deep learning model established with the above method and factors such as the network depth, network width and hyperparameters including the activation function on the EUR prediction effect of shale gas wells should be examined.

Acknowledgement

References

Alizadeh, B., Najjari, S., Kadkhodaie-Ilkhchi, A., 2012. Artificial neural network modeling and cluster analysis for organic facies and burial history estimation using well log data: a case study of the South Pars Gas Field, Persian Gulf, Iran. Comput. Geosci. 45, 261–269. https://doi.org/10.1016/j.cageo.2011.11.024.

Arns, C.H., Knackstedt, M.A., Pinczewski, M.V., et al., 2001. Accurate estimation of transport properties from microtomographic images. Geophys. Res. Lett. 28 (17), 3361–3364. https://doi.org/10.1029/2001GL012987.

Bi, H.B., Meng, H., Gao, R.L., et al., 2020. Evaluation method of recoverable reserves of single well in undeveloped area of shale gas. Acta Pet. Sin. 41 (5), 565–573. https://doi.org/10.7623/syxb202005005 (in Chinese).

David, O., Sunday, A., Faisal, K., et al., 2018. Data driven model for sonic well log prediction. J. Petrol. Sci. Eng. 170, 1022–1037. https://doi.org/10.1016/j.petrol.2018.06.072.

Dong, D.Z., Wang, Y.M., Li, X.J., et al., 2016. Breakthrough and prospect of shale gas exploration and development in China. Nat. Gas. Ind. B 3 (1), 12–26. https://doi.org/10.1016/j.ngib.2016.02.002.

Dong, D.Z., Zou, C.N., Yang, H., et al., 2012. Progress and prospects of shale gas exploration and development in China. Acta Pet. Sin. 33 (S1), 107–114. https://doi.org/10.7623/syxb2012S1013 (in Chinese).

Goodfellow, I., Bengio, Y., Courville, A., 2016. Deep Learning. The MIT Press, Cambridge, ISBN 978-0262035613.

Hector, H., Horacio, F., 2020. Data-driven prediction of unconventional shale-reservoir dynamics. SPE J. 25 (5), 2564–2581. https://doi.org/10.2118/193904-PA.

Hinton, G.E., Osindero, S., Teh, Y.W., 2006. A fast learning algorithm for deep belief nets. Neural Comput. 18 (7), 1527–1554. https://doi.org/10.1162/neco.2006.18.7.1527.

Hinton, G.E., Salakhutdinov, R.R., 2006. Reducing the dimensionality of data with neural networks. Science 313 (5786), 504–507. https://doi.org/10.1126/science.1127647.

Hornik, K.M., Stinchcomb, M., White, H., 1989. Multilayer feedforward networks are universal approximator. Neural Network. 2 (5), 355–366. https://doi.org/10.1016/0893-6080(89)90020-8.

Ismail, N.I., Latham, S., Arns, C.H., et al., 2013. Rock-typing using the complete set of additive morphological descriptors. SPE Reservoir Characterisation and Simulation Conference and Exhibition, Abu Dhabi, UAE. Society of Petroleum Engineers. https://doi.org/10.2118/165989-MS.

Ismail, N.I., 2014. Rock Typing Using the Complete Set of Additive Morphological Descriptors. The university of New South Wales, Sydney.

Iturrar, N.U., Parra, J.O., 2014. Artificial Neural Networks applied to estimate permeability, porosity and intrinsic attenuation using seismic attributes and well-log data. J. Appl. Geophys. 107 (1), 45–54. https://doi.org/10.1016/j.jappgeo.2014.05.010.

Krizhevsky, A., Sutskever, I., Hinton, G.E., 2012. ImageNet classification with deep convolutional neural networks. International Conference on Neural Information Processing Systems, Lake Tahoe, Nevada, USA. Curran Associates Inc. https://dl.acm.org/doi/10.5555/2999134.2999257.

Liu, P.G., Liu, Y.Y., Pan, M., et al., 2017a. Research of image process and phase segmentation of 3D sandstone samples based on micro-CT tomogram. Sci. Technol. Eng. 17 (6), 22–30. https://doi.org/10.3969/j.issn.1671-1815.2017.06.004 (in Chinese).

Liu, Q.B., 2020. Research on Key Methods of Tight Oil Sweet Spots Evaluation Using Deep Learning. Peking University, Beijing (in Chinese).

Liu, Y.Y., Pan, M., 2017. Research of conductivity simulation and upscaling based on 3D sandstone core sample. Sci. Technol. Eng. 17 (15), 48–56. https://doi.org/10.3969/j.issn.1671-1815.2017.15.007 (in Chinese).

Liu, Y.Y., Liu, S.Q., Pan, M., et al., 2019a. Research of crustal stress simulation using finite element analysis based on corner point grid. Acta Sci. Nauralium Univ. Pekin. 55 (4), 643–653. https://doi.org/10.13209/j.0479-8023.2019.020 (in Chinese).

Liu, Y.Y., Liu, S.Q., Pan, M., 2020. Finite element simulation of oil and gas reservoir in-situ stress based on a 3d corner-point grid model. Math. Probl Eng. 2020, 7384085. https://doi.org/10.1155/2020/7384085.

Liu, Y.Y., Ma, X.H., Zhang, X.W., et al., 2021. Shale gas well flowback rate prediction for Weiyuan field based on a deep learning algorithm. J. Petrol. Sci. Eng. 203, 108637. https://doi.org/10.1016/j.petrol.2021.108637.

Liu, Y.Y., Pan, M., Liu, S.Q., 2019b. Petrel2ANSYS: accessible software for simulation of crustal stress fields using constraints provided by multiple 3D models employing different types of grids. J. Cent. S. Univ. 26 (9), 2447–2463. https://doi.org/10.1007/s11771-019-4186-4.

Liu, Y.Y., Pan, M., Zhang, C., et al., 2017b. Research of permeability numerical prediction and upscaling based on micro-ct computed tomography of sandstone core sample. Acta Sci. Nauralium Univ. Pekin. 53 (6), 1021–1030. https://doi.org/10.13209/j.0479-8023.2017.054 (in Chinese).

Lu, H., Li, Q., Yue, D.L., et al., 2021. Study on optimal selection of porosity logging interpretation methods for Chang 73 segment of the Yanchang Formation in the southwestern Ordos Basin, China. J. Petrol. Sci. Eng. 198, 108153. https://doi.org/10.1016/j.petrol.2020.108153.

Ma, X.H., 2017a. A golden era for natural gas development in the Sichuan Basin. Nat. Gas. Ind. B 4 (3), 163–173. https://doi.org/10.1016/j.ngib.2017.08.001.

Ma, X.H., 2017b. Natural gas and energy revolution: a case study of Sichuan-Chongqing gas province. Nat. Gas. Ind. B 4 (2), 91–99. https://doi.org/10.1016/j.ngib.2017.07.014.

Ma, X.H., 2018. Enrichment laws and scale effective development of shale gas in the southern Sichuan Basin. Nat. Gas. Ind. 38 (10), 1–10. https://doi.org/10.3787/j.issn.1000-0976.2018.10.001 (in Chinese).

Ma, X.H., Xie, J., 2018. The progress and prospects of shale gas exploration and exploitation in southern Sichuan Basin, NW China. Petrol. Explor. Dev. 45 (1), 172–182. https://doi.org/10.1016/S1876-3804(18)30018-1.

Ma, X.H., Li, X.Z., Liang, F., et al., 2020b. Dominating factors on well productivity and development strategies optimization in Weiyuan shale gas play, Sichuan Basin, SW China. Petrol. Explor. Dev. 47 (3), 594–602. https://doi.org/10.1016/S1876-3804(20)60076-3.

Ma, X.H., Xie, J., Yong, R., et al., 2020a. Geological characteristics and high production control factors of shale gas reservoirs in Silurian Longmaxi Formation, southern Sichuan Basin, SW China. Petrol. Explor. Dev. 47 (5), 901–915. https://doi.org/10.1016/S1876-3804(20)60105-7.

Maas, A.L., Hannun, A.Y., Ng, A.Y., 2013. Rectifier Nonlinearities Improve Neural Network Acoustic Models. The 30th International Conference on Machine Learning, Atlanta, Georgia, USA.

Mattia, A., 2015. Seismic velocity estimation from well log data with genetic algorithms in comparison to neural networks and multilinear approaches. J. Appl. Geophys. 117, 13–22. https://doi.org/10.1016/j.jappgeo.2015.03.021.

Rolon, L., Mohaghegh, S.D., Ameri, S., et al., 2009. Using artificial neural networks to generate synthetic well logs. J. Nat. Gas Sci. Eng. 1 (4/5), 118–133. https://doi.org/10.1016/j.jngse.2009.08.003.

Salehi, M.M., Rahmati, M., Karimnezhad, M., et al., 2016. Estimation of the non records logs from existing logs using artificial neural networks. Egypt. J. Petrol. 26 (4), 957–968. https://doi.org/10.1016/j.ejpe.2016.11.002.

Shi, X., Liu, G., Cheng, Y.F., et al., 2016. Brittleness index prediction in shale gas reservoirs based on efficient network models. J. Nat. Gas Sci. Eng. 35A, 673–685. https://doi.org/10.1016/j.jngse.2016.09.009.

Silversides, K., Melkumyan, A., Wyman, D., et al., 2015. Automated recognition of stratigraphic marker shales from geophysical logs in iron ore deposits. Comput. Geosci. 77 (1), 118–125. https://doi.org/10.1016/j.cageo.2015.02.002.

Singh, U.K., 2011. Fuzzy inference system for identification of geological stratigraphy off Prydz Bay, East Antarctica. J. Appl. Geophys. 75 (4), 687–698. https://doi.org/10.1016/j.jappgeo.2011.08.001.

Tieleman, T., Hinton, G.E., 2012. Lecture 6.5-Rmsprop: divide the gradient by a running average of its recent magnitude. Coursera: Neural Netw. Mach. Learn. 4 (1), 26–30.

Wang, H.J., Wu, W., Chen, T., et al., 2019a. An improved neural network for TOC, S1 and S2 estimation based on conventional well logs. J. Petrol. Sci. Eng. 176,

664—678. https://doi.org/10.1016/j.petrol.2019.01.096.

Wang, S.H., Chen, Z., Chen, S.N., 2019b. Applicability of deep neural networks on production forecasting in Bakken shale reservoirs. J. Petrol. Sci. Eng. 179, 112—125. https://doi.org/10.1016/j.petrol.2019.04.016.

Wang, Y.C., Jiang, H.Q., Yu, F.W., et al., 2019c. Researches on the pore permeability prediction method of 3D digital cores based on machine learning. Petrol. Sci. Bull. 4 (4), 354—363. https://doi.org/10.3969/j.issn.2096-1693. 2019.04.032 (in Chinese).

Xu, E.H., 2018. Reservoir History Matching for Transit Pressure Based on Support Vector Regression. Hefei University of Technology, Hefei (in Chinese).

Yang, B., Liu, Y.Y., Pan, M., 2017. Rock-type classification based on minkowski functionals and K-means cluster Analysis. Sci. Technol. Eng. 17 (22), 63—67. https://doi.org/10.3969/j.issn.1671-1815.2017.22.010 (in Chinese).

Zerrouki, A.A., Aifa, T., Baddari, K., 2014. Prediction of natural fracture porosity from well log data by means of fuzzy ranking and an artificial neural network in Hassi Messaoud oil field, Algeria. J. Petrol. Sci. Eng. 115 (1), 78—89. https://doi.org/10.1016/j.petrol.2014.01.011.

Zhang, D.L., Wu, J.F., Zhang, J., et al., 2018. Application of the normalized production decline analysis method for shale gas of North America - taking Changning-Weiyuan Demonstration Area as an Example. Sci. Technol. Eng. 18 (34), 51—56. https://doi.org/10.3969/j.issn.1671-1815.2018.34.007 (in Chinese).

Zhang, Z., Niu, W., Hu, R.R., et al., 2020. Application of EUR rapid evaluation method for shale gas-take Zhaotong demonstration area as an example. Petrochem. Ind. Appl. 39 (9), 6—10. https://doi.org/10.3969/j.issn.1673-5285.2020.09.002 (in Chinese).

Zhao, W.Z., Jia, A.L., Wei, Y.S., et al., 2020. Progress in shale gas exploration in China and prospects for future development. China Petrol. Explor. 25 (1), 31—44. https://doi.org/10.3969/j.issn.1672-7703.2020.01.004 (in Chinese).

Zhao, Y.L., Liang, H.B., Jing, C., et al., 2019. A new method for quick EUR evaluation of shale gas wells. J. Southwest Petrol. Univ. (Sci. Technol. Ed.) 41 (6), 124—131. https://doi.org/10.11885/j.issn.1674-5086.2019.09.16.09 (in Chinese).

Zhou, J.R., 2017. Research on Auto History Matching Techniques Base on Production-Injection Profile. China University of Petroleum (East China), Qingdao (in Chinese).

Zhu, L.Q., Zhang, C., Zhang, C.M., et al., 2019. Forming a new small sample deep learning model to predict total organic carbon content by combining unsupervised learning with semisupervised learning. Appl. Soft Comput. 83, 105596. https://doi.org/10.1016/j.asoc.2019.105596.

Zhu, L.Q., Zhang, C., Zhang, C.M., et al., 2020a. A new and reliable dual model- and data-driven TOC prediction concept: a TOC logging evaluation method using multiple overlapping methods integrated with semi-supervised deep learning. J. Petrol. Sci. Eng. 188, 106944. https://doi.org/10.1016/j.petrol.2020.106944.

Zhu, L.Q., Zhang, C.M., Zhang, Z.S., et al., 2020b. High-precision calculation of gas saturation in organic shale pores using an intelligent fusion algorithm and a multi-mineral model. Adv. Geo-Energy Res. 4 (2), 135—151. https://doi.org/10.26804/ager.2020.02.03.

Zou, C.N., Dong, D.Z., Wang, Y.M., et al., 2015. Shale gas in China: characteristics, challenges and prospects (I). Petrol. Explor. Dev. 42 (6), 753—767. https://doi.org/10.1016/S1876-3804(15)30072-0.

Zou, C.N., Dong, D.Z., Wang, Y.M., et al., 2016. Shale gas in China: characteristics, challenges and prospects (II). Petrol. Explor. Dev. 43 (2), 182—196. https://doi.org/10.1016/S1876-3804(16)30022-2.

Zou, C.N., Yang, Z., Zhang, G.S., et al., 2019. Establishment and practice of unconventional oil and gas geology. Acta Geol. Sin. 93 (1), 12—23. https://doi.org/10.3969/j.issn.0001-5717.2019.01.003 (in Chinese).